Computers and Electronics in Agriculture 222 (2024) 109080

Contents lists available at ScienceDirect

Computers and Electronics in Agriculture

journal homepage: www.elsevier.com/locate/compag

Original papers

Multi-output deep learning models for enhanced reliability of simultaneous tree above- and below-ground biomass predictions in tropical forests of Vietnam

Bao Huy [a,b,*], Nguyen Quy Truong [a,1], Krishna P. Poudel [c], Hailemariam Temesgen [b], Nguyen Quy Khiem [a]

[a] Forest Resources and Environment Management Consultancy (FREM), 06 Nguyen Hong, Buon Ma Thuot, Dak Lak 630000 Viet Nam
[b] Department of Forest Engineering, Resources and Management, Oregon State University (OSU), Corvallis, OR 97333, USA
[c] Department of Forestry, Mississippi State University, P.O. Box 9681, Mississippi State, MS 39762, USA

ARTICLE INFO

Keywords:
Aboveground biomass
Additive simultaneous models
Belowground biomass
Deep learning
Tropical forest

ABSTRACT

The development and evaluation of new methods for the measurement, monitoring, and assessment of forest carbon biomass is necessary to quantify the ecosystem services provided by forests. To that end, multi-output deep learning (MODL) models were developed, cross-validated as alternative to the conventional weighted nonlinear seemingly unrelated regression (WNSUR) method for simultaneous prediction of tree aboveground biomass (*AGB)*, tree belowground biomass (*BGB)*, and total tree biomass (*TB* = *AGB* + *BGB),* while ensuring additivity, in two main tropical forest types – Dipterocarp Forest (DF) and Evergreen Broadleaf Forest (EBLF). A destructive sample of 175 trees was collected from 27 purposively selected plots in the Central Highlands ecoregion of Vietnam. The potential predictors of *AGB, BGB* and *TB* included four tree-level variables (diameter at breast height, *DBH;* tree height, *H;* wood density, *WD;* and crown area, *CA*), three stand-level variables (*Forest type*; basal area, *BA;* and stand density, *N),* and five environmental variables (mean annual rainfall, *P;* mean annual temperature, *T; Soil type*; *Altitude;* and *Slope*). The model utilizing *DBH, CA, H, WD, BA, Altitude, P,* and *Forest type* as predictors performed the best among the MODL models developed in this study. Compared to WNSUR models that used the same set of predictors and the dataset from the same forest types of DF or EBLF, the MODL models reduced the mean absolute percent error of tree *AGB, BGB,* and *TB* by up to 24.7 %, 96.5 %, and 9.4 %, respectively. The results suggest that the MODL algorithm can be applied on a diverse spatial scale, covering gradients of forest stand characteristics, climate conditions, soil properties, and topography, as it can incorporate complex numerical and categorical variables into the models without requiring a priori functions.

1. Introduction

Forest ecosystems play a crucial role in the global carbon cycle, encompassing five primary carbon pools: aboveground plant biomass, below-ground plant biomass, litter, deadwood, and soil organic carbon (IPCC, 2006), which both sequester and release carbon simultaneously (Newell and Vos, 2012). Consequently, forest carbon optimization and management strategies are frequently incorporated into climate mitigation policy proposals (Hoover and Riddle, 2020). Among these pools, tree aboveground biomass (*AGB*) and tree below-ground biomass (*BGB)* are the most significant, accounting for approximately 31 % of the total forest carbon sequestration (Hoover and Riddle, 2020). For developing countries to participate in the Reducing Emissions from Deforestation and Forest Degradation (REDD +) program or to receive Carbon Payments for Forest Environmental Services (C-PFES), it is also necessary to provide a transparent and accurate prediction of changes in *AGB* and *BGB* over time (Pelletier et al., 2012). Therefore, the development and evaluation of new approaches, such as multi-output deep learning (MODL) models, which have the potential to enhance the reliability of simultaneous predictions of tree *AGB, BGB* and total (*TB* = *AGB* + *BGB*),

* Corresponding author.
E-mail addresses: BaoHuy.frem@gmail.com (B. Huy), QuyTruong.Ng@gmail.com (N. Quy Truong), Krishna.Poudel@msstate.edu (K.P. Poudel), Temesgen.Hailemariam@oregonstate.edu (H. Temesgen), QuyKhiem.frem@gmail.com (N. Quy Khiem).
[1] Joint first author: Nguyen Quy Truong.

https://doi.org/10.1016/j.compag.2024.109080
Received 4 December 2023; Received in revised form 14 May 2024; Accepted 19 May 2024
Available online 24 May 2024

ensuring additivity, compared to conventional allometric modeling is important.

Although *BGB* constitutes a significant portion of forest biomass (Magalhaes, 2015; Brahma et al., 2021), most studies related to forest biomass and carbon have focused on tree *AGB* (Kralicek et al., 2017; Güner et al., 2022) due to the high cost and time required to measure *BGB* of large trees (Brahma et al., 2021). Because *BGB* is linked to *AGB* dynamics (Walker et al., 2016; Brahma et al., 2021), the root-to-shoot ratio (RSR) has been commonly used to convert *AGB* to *BGB* (FAO, 2008; Walker et al., 2016). Direct equations for *BGB* have also been developed for some forest types. Kenzo et al. (2009) focused on tropical secondary forests in Malaysia, specifically developing a model for tree *BGB* estimation. Kachamba et al. (2016) developed separate models for tree *AGB* and *BGB* in the Miombo woodlands of Malawi. Kralicek et al. (2017) addressed the simultaneous estimation of tree *AGB* and *BGB* in tropical Dipterocarp Forest (DF) and Evergreen Broadleaf Forest (EBLF) in Vietnam. Furthermore, species-specific *BGB* models have been proposed by Razakamanarivo et al. (2012) for *Eucalyptus* in Madagascar, Marziliano et al. (2015) for *Phillyrea latifolia* L. in Mediterranean forest landscapes, and Magalhaes (2015) for *Androstachys johnsonii* Prain in Mozambique. Koala et al. (2017) demonstrated that species-specific *BGB* models outperformed generic allometric equations.

One of the fundamental considerations in estimating tree biomass is to account for biological relationships and ensure the additivity of component biomass (Affleck and Dieguez-Aranda, 2016; Huy et al., 2019). The seemingly unrelated regression (SUR) method (Parresol, 2001) is commonly employed to meet this requirement. The weighted nonlinear SUR (WNSUR) approach is utilized when heteroscedasticity needs to be addressed. These methods have been widely used to establish a modeling system to simultaneously predict component biomass while ensuring additivity (Kralicek et al., 2017; Huy et al., 2019; Brahma et al., 2021; Xu and Zhang, 2022). Furthermore, studies have shown that using additive equations for biomass estimation yields more reliable results than the separately fitted equations for total tree biomass and its components (Huy et al., 2019).

The conventional regression method, in general, and the WNSUR approach, often require selecting appropriate equation forms and assuming specific statistical properties such as normal distribution and homogeneous variance of errors. Consequently, limitations arise in dealing with multicollinearity, parameter estimation, model selection, and determining variance structure, leading to biased estimates (Huy et al., 2022; Xu and Zhang, 2022). Additionally, errors obtained from simultaneous *AGB, BGB*, and total *TB* prediction using the WNSUR approach are still high. For example, mean absolute percent errors (MAPE) of WNSUR modeling systems that simultaneously predict tree *AGB, BGB* and *TB* in the DF were 29 %, 50 %, and 23 %, whereas in the EBLF were 37 %, 122 % and 20 %, respectively (Kralicek et al., 2017). Therefore, several machine learning (ML) methods have been proposed as alternatives to the conventional regression models in the recent years (Xu et al., 2022).

ML encompasses algorithms that enable computers to learn from data without direct programming. Deep learning (DL), a subset of ML, utilizes deep neural networks (DNNs) and effectively models intricate patterns. The deep architecture of DNNs facilitates exploration of complex structures within datasets. DL has consistently outperformed traditional ML techniques across domains, learning intricate patterns directly from data without predefined assumptions (LeCun et al., 2015; Zhou and Feng, 2019). DL models utilize DNNs composed of multiple hidden layers that progressively extract representations (Chollet, 2018; Huy et al., 2022). These models aim to establish a functional relationship between responses and covariates based on given inputs, enabling them to address real-time problem-solving tasks (Huy et al., 2022).

DL methods have demonstrated considerable potential in uncovering complex relationships within forest ecosystems (Christin et al., 2019). These methods have proven effective in analyzing various components such as plant density, plant biomass, and organic carbon storage (Wang, 2023), positioning DL approaches as viable alternatives to conventional regression methods in biometric research, particularly in forest biomass prediction. Despite these advantages of DL models tailored for biometric research in tropical forests over conventional regression approaches (Huy et al., 2022) have not received adequate attention, particularly within the realms of forest biomass. Literature in this area remains sparse, with several DL models developed for predicting singular outputs such as tree height (*H*) (Ogana and Ercanli, 2021), crown width (Qin et al., 2023), and tree *AGB* (Huy et al., 2022). Therefore, the development of MODL models, capable of predicting tree *AGB, BGB* and total tree TB simultaneously, while ensuring additivity, will support the current need of quantifying carbon in different forest carbon pools. This study will contribute to the growing body of literature in the application of new algorithms in forestry science and document the potential of MODL in improving the reliability of *AGB* and *BGB* simultaneous estimates in tropical forests.

We hypothesize that MODL models will produce superior predictions compared to conventional simultaneous modeling systems using WNSUR, given that both approaches can simultaneously predict tree *AGB, BGB*, and *TB*. The objectives of this study were to 1) develop a MODL model system to simultaneously predict tree *AGB, BGB,* and *TB,* ensuring additivity in the tropical EBLF and DF, and 2) cross-validate the errors of MODL compared with WNSUR using the same dataset and predictors in the same forest type.

2. Materials and methods

2.1. Study sites

The study was conducted in the Central Highlands ecoregion, which has the highest tropical forest cover of the eight ecoregions in Vietnam and focused on Vietnam's main tropical forest types, namely DF and EBLF (Fig. 1). Both types of forests exhibit intricate structural characteristics, showcasing a diverse array of age groups and species mixture. Dipterocarpaceae stands out as the predominant plant family in the DF but the EBLF lacks dominance by any singular plant family, yet species from Fagaceae, Myrtaceae, and Lauraceae families are prevalent (Kralicek et al., 2017). Table 1 summarizes the ecological factors and variables of the forest stand in the study area.

2.2. Data

The dataset used in this study was obtained from Kralicek et al. (2017). Twenty-seven sample plots were located in two forest types: DF (13 plots; 50 × 50 m) and EBLF (14 plots; 20 × 100 m). In each plot, species names and diameter at breast height (*DBH*, cm) was recorded for all trees larger than 5 cm in *DBH* and a set of trees was chosen for destructive sampling, prioritizing the dominant species in each forest type and reflected the diameter distribution observed in the stands. In total, 175 trees were destructively sampled, encompassing 48 species, 40 genera, and 28 families. Among these, 105 sampled trees belonged to DF, while 70 sampled trees were from the EBLF.

For tree *AGB* data, the selected trees were cut down. Prior to cutting them down, we determined the species name, measured *DBH*, and measured the crown diameter (*CD*) by averaging two measurements taken in the cardinal directions. Tree *H* was measured after the trees had been felled. The fresh *AGB* of the destructively sampled trees was divided into its components: the stem with bark, branches, and leaves (Huy et al., 2016a; Huy et al., 2016b). For tree *BGB* data, we used the root excavation method, a commonly employed standard technique as demonstrated by Marziliano et al. (2015), Röhling et al. (2019), and Medrano-Meraz et al. (2021). However, it's worth noting that the implementation of this method was both time-consuming and expensive. Achieving precise measurements of fresh root biomass for trees in tropical uneven-aged and mixed-species forests presented significant hurdles. Consequently, we invested substantial efforts and resources into

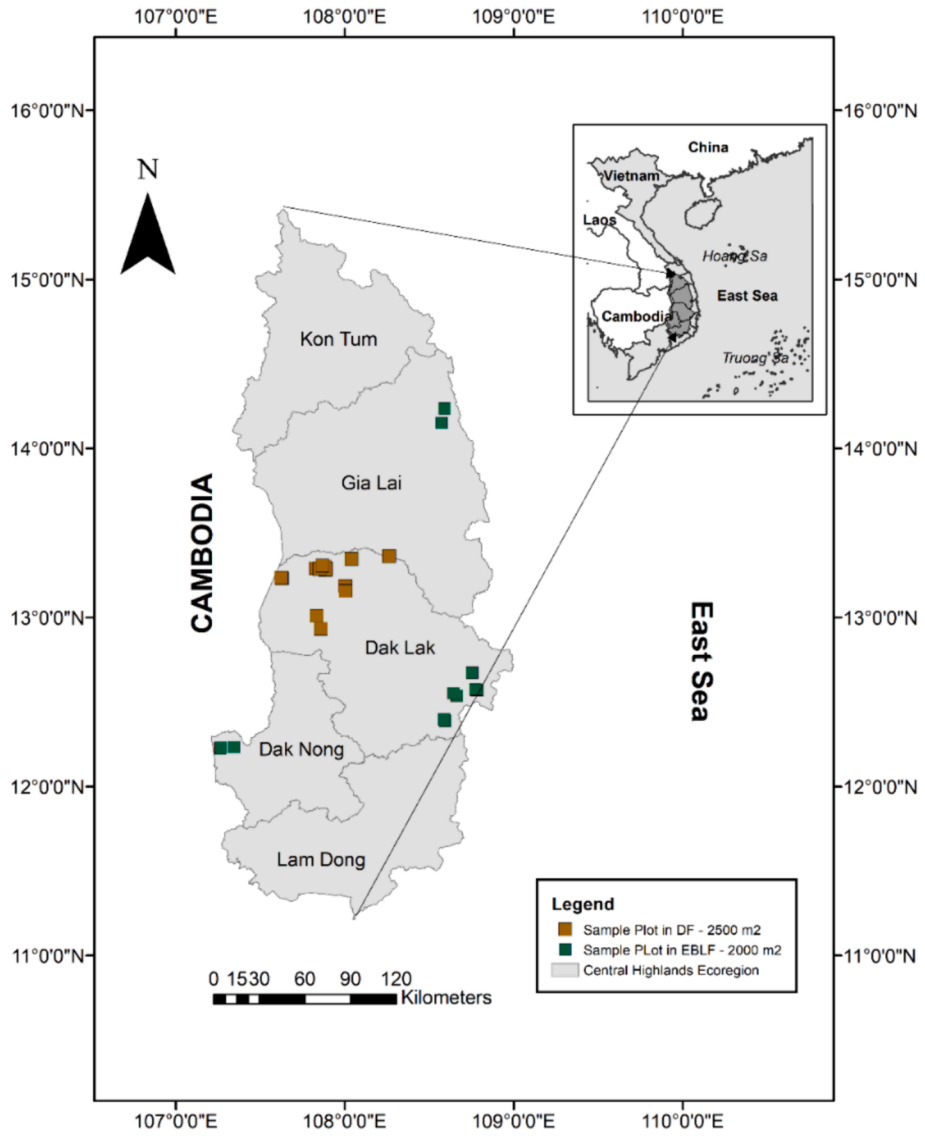

Fig. 1. Locations of sample plots for the Dipterocarp Forest (DF) and the Evergreen Broadleaf Forest (EBLF) in the Central Highlands ecoregion of Vietnam.

gathering root biomass data for the 175 sample trees across two tropical forest types, DF and EBLF, ensuring the reliability required for constructing estimation models for *BGB*. The root systems of all sample trees were fully excavated, and measurements were recorded for roots with a diameter exceeding 2 mm (IPCC, 2006). Fine roots with a diameter of less than 2 mm were excluded due to their contribution to other biomass pools such as soil organic matter or litter (Rohling et al., 2019; IPCC, 2006). Industrial vehicles were indispensable for extracting the root systems of large trees, whereas the remaining roots, including those of smaller trees, were dug up manually. Subsequently, excavation along each individual coarse root was carried out until the entire root structure was exposed.

The fresh weight of tree components (leaves, branches, stem with bark, and roots) was also recorded in the field using an electronic scale with a precision of 0.05 kg. To calculate the fresh-to-dry mass ratio of each component, we carefully packaged samples and transported them to the laboratory for analysis. For each sampled tree, roots were categorized into three size groups (large, medium, and small) based on the tree's diameter. Approximately 300 g of root samples were collected from these three categories. Wood samples (500 g), bark samples (300 g), and wood disks for wood density (*WD*) calculations were collected at five replications along the stem of each tree. Additionally, three branch samples (500 g each) were collected for each tree: one from the largest branch, one from a medium-sized branch, and one from the smallest branch. Furthermore, two foliage samples (300 g each) of new and old leaves were collected for each tree (Kralicek et al., 2017). All component samples were weighed for fresh biomass on site using an electronic scale with a precision of 0.01 g.

The fresh volume of wood samples was determined in the laboratory using the water displacement method. Subsequently, all samples were chipped into small pieces and dried at 105 °C until a constant weight was attained. The total above- and below-ground dry weights of a tree (*AGB, BGB*, respectively) were calculated by multiplying the fresh weight of each component by its respective fresh-to-dry ratio and summing across the relevant components. The *WD* of a sample was calculated as the ratio of the dry weight to the fresh volume of each sample, while the *WD* of a sample tree was computed as the arithmetic average of the *WD* values of all samples from that particular tree (Kralicek et al., 2017).

The variables included in the dataset were as follows: 1) response variables: tree *AGB,* representing the total dry biomass of stem, bark, branches, and leaves; tree *BGB*, representing the dry biomass of the tree root system; the total dry biomass of each sampled tree (*TB*) was calculated as the sum of *AGB* and *BGB* ($TB = AGB + BGB$); 2) tree level predictors: *DBH,* tree crown area (*CA*) calculated based on averaged *CD*

Table 1
Summary statistics of variables.

ID	Variables	Min	Mean	Max	Std.
Response variables:					
1	*AGB* (kg tree^{-1})	1.5	54.7	993.5	113.7
2	*BGB* (kg tree^{-1})	0.5	11.2	172.6	19.4
3	*TB* (kg tree^{-1})	2.6	66.0	1166.1	131.7
Predictive variables:					
	Tree variables:				
4	*DBH* (cm)	3.4	10.9	40.5	5.9
5	*CA* (m^2 tree^{-1})	0.38	8.13	54.11	8.09
6	*H* (m)	2.8	8.7	19.0	3.3
7	*WD* (g cm^{-3})	0.354	0.611	0.912	0.107
	Stand variables:				
8	*Forest type* (categorical variable):	Dipterocarp Forest (DF) and Evergreen Broadleaf Forest (EBLF)			
9	*BA* (m^2 ha^{-1})	7.00	23.65	49.00	13.48
10	*N* (trees ha^{-1})	256	879	3330	572
	Ecological variables:				
11	*P* (mm year^{-1} averaged)	1600	1846	2500	320
12	*T* (^{0}C averaged)	22.2	24.9	25.5	1.0
13	*Soil type* (categorical variable):	Igneous rocks and Sedimentary rocks			
14	*Altitude* (m)	197	448	1068	255
15	*Slope* (degree)	0.0	6.9	36.0	10.7

Note: *AGB*: Aboveground biomass, *BGB*: Below-ground biomass, *TB*: Total biomass including tree above- and belowground biomass, *DBH*: Diameter at breast height, *CA:* Tree crown area, *H*: Tree height, *WD*: Wood density, *BA:* Stand basal area, *N*: Stand density, *P*: Mean annual precipitation, *T*: Mean annual temperature.

using the formula $CA = \pi/4 \times CD^2$, tree *H*, and *WD*; 3) stand attributes and environmental factors: basal area (*BA*), stand density (*N*), and *Forest type*; mean annual rainfall (*P*) and mean annual temperature (*T*) (Fick and Hijmans, 2017); *Soil types* (Fischer et al., 2008), along with *Altitude,* and *Slope*. Table 1 provides a summary of the statistics of these variables.

2.3. Variable selection

Various methods are available to select variables for analyzing relationships, including Principal Component Analysis (PCA), Factor Analysis for Mixed Data (FAMD), and model selection by exhaustive search, forward or backward stepwise, or sequential replacement. The PCA can accommodate continuous numerical variables but is not suited for datasets containing mixed numerical and categorical variables. Regression model selection, on the other hand, might not provide a straightforward interpretation of factors. FAMD is specifically tailored to handle datasets encompassing both numerical and categorical variables. Its application aids in reducing predictive variables while enhancing the interpretability of multiple factors. In the FAMD approach, variables are normalized to ensure equal influence from numerical and categorical variables (Huy et al., 2022; R Core Team, 2023). Given that our dataset incorporates both numerical and categorical variables, we employed FAMD, following the approach outlined by Huy et al. (2022), to identify the factors that contribute the most significantly to the variations in tree *AGB, BGB,* and *TB*. The FAMD was implemented using the FAMD package in R version 4.0.5 (R Core Team, 2023).

2.4. Multi-output deep learning (MODL)

MODL models map each input to multiple outputs simultaneously. By employing DL techniques to predict multiple response outputs based on input variables, which include both observed response variables and predictive observed covariates, it is possible to address significantly more complex decision-making problems (Xu et al., 2020). Suppose $X = R^z$ is a z-dimensional input space and $Y = R^m$ is an m-dimensional output space. MODL aims to learn a function $F: X \times Y \rightarrow R$ based on the training dataset D of input response and predictive variables. Where $D = \{(x_i, y_i) | 1 \leq i \leq n\}$ with $x_i \in X$ is a z-dimensional input vector, and $y_i \in Y$ is an m-dimensional output vector associated with x_i. The aim is to predict the output response variables in one instance simultaneously. Multiple outputs are associated with each instance, represented by a real-valued vector, where the values represent how closely the instance corresponds to a response. Therefore, the learned multi-objective function that predicts a real-valued vector is the multi-output $f(x) \in Y$ (Xu et al., 2020).

The DL models typically comprise an input layer with response variables and predictive covariates, hidden layers with neurons, and an output layer for predicting the response variable. Through iterative process across multiple hidden layers, features are progressively extracted and passed to subsequent layers, enabling the discovery of complex relational functions among input variables and covariates (LeCun et al., 2015; Ogana and Ercanli, 2021; Huy et al., 2022).

The transformation within the DNN is carried out by a layer that is parameterized by its weights. This deep learning process involves determining the appropriate values for the weights across all layers of the DNN. In this study, to enable simultaneous predictions of multi-response variables, the DNN learning process for weight determination (Huy et al., 2022) was modified as follows:

$$y_{m\,product\,1} = \sum_{i=1}^{z} X_i \times w_i + \varepsilon_1 \tag{1}$$

$$Y_{m\,product} = \left[y_{m\,product\,1}, y_{m\,product\,2}, \cdots, y_{m\,product\,ne} \right] \tag{2}$$

$$y_{m\,output\,1} = f\left(\sum_{i=1}^{z} X_i \times w_i + \varepsilon_1 \right) \tag{3}$$

$$Y_{m\,output} = \left[y_{m\,output\,1}, y_{m\,output\,2}, \ldots, y_{m\,output\,ne} \right] \tag{4}$$

where $y_{m\,product\,ne}$ is the m multi-product of the input vector $X = [X_1, X_2, \ldots X_i., X_z]$, z is the number of input variables, and w_i is the weight on interconnection along with X_i and ε_i is the bias value, *ne* is the number of neurons of the network, $Y_{m\,product}$ is the m multi-product vector, f is the activation function used at the neuron, and $y_{m\,output\,ne}$ is the m multi-output of the neuron and $Y_{m\,output}$ is the m multi-output vector.

Like other single-output DL models (Huy et al., 2022), MODL models in this study also utilize DNNs. However, the DNNs, akin to the SUR method, are tailored to produce an output layer facilitating simultaneous prediction of response variables while accounting for the correlation among the errors of component models (Seely et al., 2023). This design ensures additivity within the model systems, enabling simultaneous prediction of multiple outputs and contributing to error reduction within the model framework.

A specific loss function was designed to regulate the output of DNN for MODL models, mean absolute percent error was used as the loss function ($MAPE_{loss}$, %) to control the percentage deviation in the simultaneous prediction of tree *AGB, BGB,* and *TB* within MODL models. The $MAPE_{loss}$ involves 53 validation samples accounting for 30 % of the randomly split dataset, designed to ensure harmonization of the errors between the simultaneously predicted *AGB* and *BGB* components, thereby achieving the smallest error possible for the total *TB* prediction. The $MAPE_{loss}$ devised in this study also guarantees that the total prediction aligns closely with the actual observed values. It further captures the error reduction for each component while maintaining an overall balance.

$MAPE_{AB\_loss}$ serves as the loss function for making simultaneous predictions of *AGB,* and *BGB* is defined as:

$$MAPE_{AB\_loss}(\%) = \frac{100}{m} \sum_{i=1}^{m} \left\{ \left| \frac{y_{ai} - \hat{y}_{ai}}{y_{ai}} \right| + \left| \frac{y_{bi} - \hat{y}_{bi}}{y_{bi}} \right| \right\} \tag{5}$$

Similarly, $MAPE_{T\_loss}$ acts as an additional constraint, ensuring that the predicted total tree biomass *TB* matches the combined sum of

observed *AGB* and *BGB* components and is defined as:

$$MAPE_{T\_loss}(\%) = \frac{100}{m}\sum_{i=1}^{m}\left|\frac{(y_{ai}+y_{bi})-(\hat{y}_{ai}+\hat{y}_{bi})}{y_{ai}+y_{bi}}\right| = \frac{100}{m}\sum_{i=1}^{m}\left|\frac{y_{ti}-\hat{y}_{ti}}{y_{ti}}\right| \quad (6)$$

The overall loss function is denoted as $MAPE_{loss}$:

$$MAPE_{loss(\%)} = MAPE_{AB\_loss} + MAPE_{T\_loss}$$

$$= \frac{100}{m}\sum_{i=1}^{m}\left\{\left|\frac{y_{ai}-\hat{y}_{ai}}{y_{ai}}\right| + \left|\frac{y_{bi}-\hat{y}_{bi}}{y_{bi}}\right| + \left|\frac{y_{ti}-\hat{y}_{ti}}{y_{ti}}\right|\right\} \quad (7)$$

where y_{ai}, y_{bi}, y_{ti} and $\hat{y}_{ai}$, $\hat{y}_{bi}$, $\hat{y}_{ti}$ were observed, and simultaneously predicted tree *AGB, BGB, TB* for the i^{th} sampled tree, respectively; m was the total number of observed/predicted values from the validation dataset.

The DNN architecture, developed by Huy et al. (2022), was upgraded in this study to develop a DNN capable of simultaneously predicting tree *AGB, BGB*, and *TB,* while ensuring additivity. The DNN was trained using input data layers comprising the observed tree *AGB, BGB*, and TB, and various combinations of tree-level variables, forest stand characteristics, ecological factors, and environmental factors were identified using the FAMD method. The one-hot encoding technique in TensorFlow's tf.one_hot() function (TensorFlow, 2023) was utilized to encode categorical variables as inputs for the DNN learning process. All numeric input covariates were scaled to ensure equalization of their effects in the DNN learning process. This was achieved by dividing each variable by its maximum value and scaling it to the range [0, 1] (Huy et al., 2022). The DNN processed the information through hidden layers with hundreds of neurons and generated a multi-output layer that simultaneously predicted tree *AGB, BGB*, and *TB* while ensuring additivity. Fig. 2 illustrates the DNN architecture designed for this study.

Through the primary analysis, the optimal architecture of the DNN was selected, so that MODL models were able to simultaneously predict tree *AGB, BGB,* and *TB* while ensuring additivity, such as the numbers of hidden layers, the numbers of neurons, the hyperparameters of the epoch, the batch size and the stop function with patience (Table 2). The optimal DNN architecture consisted of multi-input variables, three hidden layers including 128 neurons in each layer, and a multi-output layer (Fig. 2). The number of epochs, a hyperparameter in DNN, specifies the number of times the DNN iterates through the entire training dataset (Huy et al., 2022). This study set the number of epochs to 3000, indicating that the DNN was trained by going through the entire dataset 3000 times. On the other hand, the batch size, another hyperparameter, determines the number of samples processed before updating the internal model parameters (Huy et al., 2022). In this specific scenario, a batch of 32 was chosen, meaning that the DNN processed 32 samples at a time before updating its parameters. In this study, with 122 training samples accounting for 70 % of the randomly split dataset, each epoch consisted of 4 batches (calculated as 122 divided by the batch size of 32). The DNN learning process underwent a maximum of 12,000 batches throughout the training dataset, calculated as four batches per epoch

Table 2
Examination of architecture and hyperparameters of the Deep Neural Network (DNN) for Multi-Output Deep Learning (MODL). The selection of the architecture and hyperparameters of the DNN was based on the errors obtained through cross-validation.

ID	Architecture /Hyperparameter	Min	Max	Step	Selected
1	Number of hidden layers	2	5	1	3
2	Number of neurones in each hidden layer	$32 = 2^5$	$512 = 2^9$	2^n with n = 5, 6, 7, 8, 9	$128 = 2^7$
3	Epoch numbers	500	5000	500	3000
4	Batch (sample size)	$32 = 2^5$	$64 = 2^6$	2^n with n = 5, 6	$32 = 2^5$
5	Patience	500	1000	500	1000

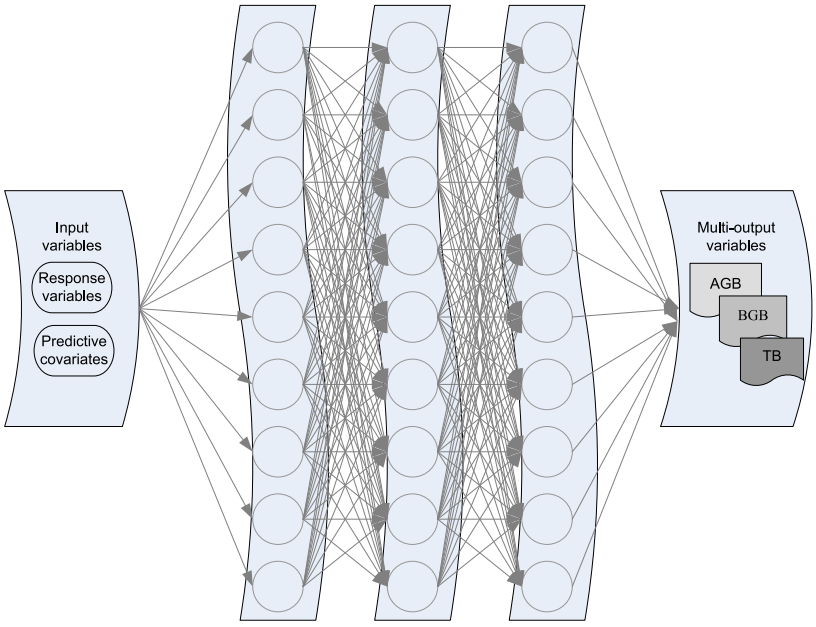

Fig. 2. Deep Neural Network (DNN) architecture for Multi-Output Deep Learning (MODL) to simultaneously predict tree above- and belowground biomass and total (*AGB, BGB*, and *TB*, respectively).

multiplied by 3000 epochs.

The DNNs employed the Adam optimization algorithm (Keras, 2022) for MODL models. For the hidden layers, the widely used Rectified Linear Unit (ReLU) activation function (Nair and Hinton, 2010; Alzubaidi et al., 2021) was utilized, as it plays a crucial role in capturing complex non-linear relationships between tree biomass responses and various predictive covariates. We applied linear activation function (Keras, 2022) for the output layer of the DNN. This choice of activation function facilitated the effective selection of the best fit between the actual and predicted output values. We implement an early stopping function to prevent overfitting with a patience value 1000 (Huy et al., 2022). This function halted the training process when the validation loss did not improve further, ensuring that the model did not become overly specialized to the training data. Furthermore, we incorporated a dropout layer of 0.5 into the DNN architecture. This dropout layer randomly deactivates 50 % of the neurons during training as a regularization technique to mitigate overfitting (Huy et al., 2022).

In this study, the application programming interfaces (APIs), Keras (Keras, 2022) and TensorFlow libraries (Chollet, 2018; Huy et al., 2022; TensorFlow, 2023) were used for MODL. MODL modeling systems were developed and cross-validated using the open-source Python programming language (Python, 2022) through custom-written codes.

2.5. Cross-validation for multi-output deep learning

A robust cross-validation process was implemented to rigorously evaluate and select the most optimal MODL models capable of simultaneously predicting tree *AGB, BGB*, and *TB* while ensuring additivity. The dataset was randomly divided ten times into two subsets: 70 % for training and 30 % for validation, ensuring an unbiased evaluation. The Fit Index (FI) was employed as a goodness-of-fit statistic to assess the models' performance, with a higher FI value approaching 1, signifying the most accurate fit to the data. Furthermore, an array of comprehensive error metrics, including bias, root mean square error (RMSE), root mean square percent error (RMSPE), and mean absolute percent error (MAPE), were calculated to evaluate the models' overall performance.

$$FI = \frac{1}{k}\sum_{1}^{k}\left(1 - \frac{\sum_{i=1}^{m}(y_i - \hat{y}_i)^2}{\sum_{i=1}^{m}(y_i - \bar{y})^2}\right) \tag{8}$$

$$Bias(\%) = \frac{1}{k}\sum_{1}^{k}\frac{100}{m}\sum_{i=1}^{m}\frac{y_i - \hat{y}_i}{y_i} \tag{9}$$

$$RMSE\left(kg\,tree^{-1}\right) = \frac{1}{k}\sum_{1}^{k}\sqrt{\frac{1}{m}\sum_{i=1}^{m}(y_i - \hat{y}_i)^2} \tag{10}$$

$$RMSPE(\%) = \frac{1}{k}\sum_{1}^{k}100\sqrt{\frac{1}{m}\sum_{i=1}^{m}\left(\frac{y_i - \hat{y}_i}{y_i}\right)^2} \tag{11}$$

$$MAPE(\%) = \frac{1}{k}\sum_{1}^{k}\frac{100}{m}\sum_{i=1}^{m}\left|\frac{y_i - \hat{y}_i}{y_i}\right| \tag{12}$$

where k represents the number of realizations, which in this case was 10; m denotes the number of sampled trees in the validation dataset; and y_i, $\hat{y}_i$ and $\bar{y}$ represent the observed, predicted, and averaged values of tree *AGB*, *BGB* and *TB* for the i^{th} validated tree in the k^{th} realization.

Graphical analysis was employed to assess the model performance, specifically examining the trend of fitted values versus observed values and the residuals versus fitted values for each modeling system. These plots provided valuable insights into the accuracy and appropriateness of the models. Once the best MODL models were validated and identified based on the function loss, they were saved within the Python code for future use. Subsequently, the Python code will utilize these saved models to make simultaneous predictions of tree *AGB, BGB*, and *TB*.

3. Results

3.1. Input variables for deep neural network

The FAMD result shown in Fig. 3 indicates the extent to which a variable contributes to the overall variability observed in the dataset. Variables with higher contributions are considered more influential in driving the observed patterns, while those with lower contributions have less impact. Among the variables under consideration, *TB, AGB, BGB, DBH, CA,* and *H* made the highest contributions – exceeding the mean contribution level – to the overall variability observed in the dataset, as illustrated in Fig. 3. In contrast, variables such as *Soil type, T, Slope*, and *N* exhibited the lowest contributions and were consequently excluded from further analysis. The remaining 11 factors, comprising three response variables (*TB, AGB,* and *BGB*) and eight predictive covariates (*DBH, CA, H, WD, BA, Altitude, P,* and *Forest type*), were utilized in the deep neural network.

3.2. Multi-output deep learning models for simultaneously predicting AGB, BGB and TB

Nine MODL models were developed in two forest types, DF and EBLF (Table 3), using different combinations of predictive covariates selected through FAMD. To evaluate the performance of these models, plots of fitted versus observed values and residuals versus fitted values were generated and presented in Fig. 4. These plots provide information on the accuracy and precision of the model's predictions. Furthermore, Table 3 presents the cross-validation statistics for each model. These statistics serve as metrics to assess the performance and effectiveness of the developed MODL models in predicting biomass variables.

In Table 3, MODL models had combinations of 2 predictive variables (*DBH, Forest type*) to up to 8 predictive variables (*DBH, CA, H, WD, BA, Altitude, P, Forest type*). Variable *Forest type* was included in all models to distinguish the tree *AGB, BGB* and *TB* predictions for each forest type such as DF and EBLF. As expected, the MODL model had higher reliability and lower errors as predictive variables increased from two to eight (Table 3 and Fig. 4). In particular, the model with 5 predictors – *DBH, CA, H, WD*, and *Forest type* – exhibited cross-validation statistical metrics comparable to the optimal model with 8 predictors (Table 3). Additionally, the MODL model with 4 predictors – *DBH, H, WD,* and *Forest type* – demonstrated higher levels of efficiency in the plots compared to other models (Fig. 4). However, these models have limitations in their applicability due to their exclusive focus on predictors at the tree level, while lacking consideration of stand-level and ecological environmental variables. As a result, they were not selected as the optimal model. The optimal MODL model, comprising 8 predictors – *DBH, CA, H, WD, BA, Altitude, P,* and *Forest type* – yielded the best simultaneous predictions of the tree *AGB, BGB* and *TB,* while ensuring additivity in both forest types of DF and EBLF; where FI = 0.875, 0.791, 0.922, and MAPE = 16.42 %, 29.01 %, 14.90 % for the simultaneously predicted tree *AGB, BGB, TB*, respectively.

The study also developed eight MODL models to simultaneously predict tree *AGB, BGB,* and *TB* for the DF using 1 predictor (*DBH*) to a maximum of 6 predictor variables (*DBH, CA, H, WD, BA, Altitude)* (Table 4). The *P* factor was excluded because the distribution of the DF falls within the same range as the *P* values. Based on cross-validation statistics and errors (Table 4), the MODL model with four optimal predictor variables *DBH, CA, H,* and *WD* provided the best simultaneous predictions of tree *AGB, BGB,* and *TB* while ensuring additivity in DF; where FI = 0.981, 0.719, 0.965, and MAPE = 13.22 %, 27.72 %, 10.95 % for simultaneously predicted tree *AGB, BGB, TB*, respectively.

Nine MODL models were also developed to simultaneously predict tree *AGB, BGB*, and *TB,* ensuring additivity for the EBLF (Table 5). These models utilized a range of predictors, varying from one predictor (*DBH*) up to a maximum of seven predictor variables (*DBH, CA, H, WD, BA, Altitude,* and *P*), as outlined in Table 5. After cross-validation, the MODL

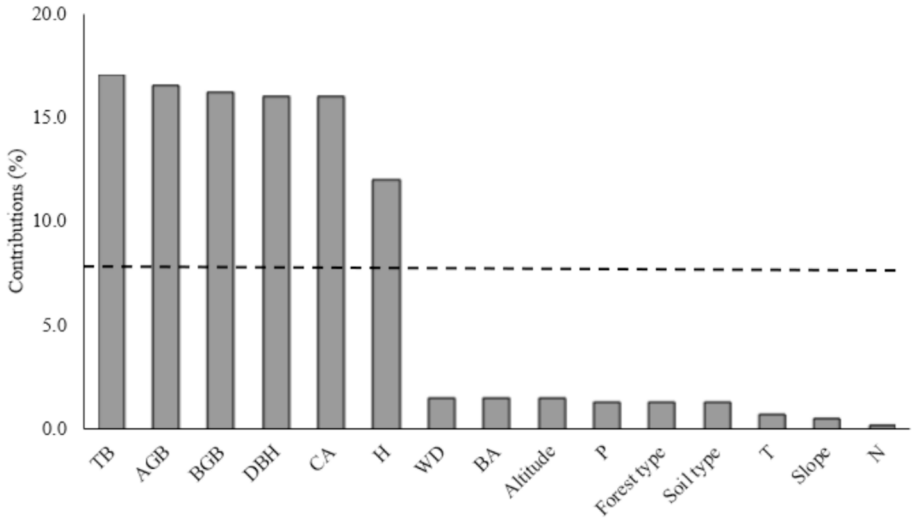

Fig. 3. Contributions of mixed numerical and categorical variables to the overall variability observed in the dataset in Factor Analysis for Mixed Data (FAMD). The dashed line represents the mean contribution level.

model incorporating three optimal predictor variables – *DBH, H,* and *WD* – demonstrated the most accurate simultaneous predictions for tree *AGB, BGB,* and *TB* ensuring additivity in the EBLF. Notably, the performance indices were recorded as follows: FI = 0.884, 0.684, and 0.947, while the corresponding MAPE values were 12.44 %, 25.60 %, and 10.56 % for the simultaneous predictions of tree *AGB, BGB*, and *TB*, respectively.

Through the comparison between MODL models for simultaneous predictions of tree *AGB, BGB,* and *TB,* including both DF and EBLF forest types (Table 3) and MODL models for each forest type such as DF and EBLF (Table 4 and Table 5), the results showed significant difference through cross-validation. The optimal MODL models developed specifically for each forest type exhibited higher accuracy than those designed collectively for both types.

This study also developed single-output deep learning models to separately predict tree *AGB, BGB*, and *TB* (Table 6) in two forest types, DF and EBLF and compared to those of the MODL models for simultaneous estimations of tree *AGB, BGB*, and *TB* while ensuring additivity (Table 3) with the same combinations of predictive variables. The cross-validation statistical metrics of the MODL models, designed for simultaneous estimations, were approximately comparable to those of the single-output DL models used for separate estimations of tree *AGB, BGB*, and *TB* (Table 3 vs. Table 6). Specifically, the MAPE for predicting *TB* while ensuring additivity in both forest types, DF and EBLF, using the optimal MODL was significantly lower at 14.90 % (Table 3) compared to the single-output DL model with the same set of 8 predictive covariates, which had a MAPE of 17.59 % (Table 6).

As a result, simultaneous prediction with MODL models harmonized the error between tree *AGB* and tree *BGB* estimates, thereby providing a better *TB* estimate compared to the separate *TB* estimation of a single-output DL model (Table 3 vs. Table 6). In addition, the MODL models for simultaneous estimations of tree *AGB, BGB*, and *TB* also ensure the additivity of the tree component biomass and the total as the SUR method does.

4. Discussion

4.1. Comparison of MODL and WNSUR

The SUR method (Parresol, 2001; Sanquetta et al., 2015; Poudel and Temesgen, 2016) was initially employed because it ensures the additivity of biomass components to total tree biomass. Additionally, weighted nonlinear models were utilized to account for the heterogeneity of errors (Huy et al., 2016a,b, 2019). WNSUR was performed using the SAS Proc Model procedure with the generalized least squares (GLS) method (SAS Institute Inc. 2014). The WNSUR modeling system employed a popular power-law function for each component equation (Brahma et al., 2021), with the following general form (Kralicek et al., 2017; Huy et al., 2019):

$$AGB_i = \alpha_1 X_{1i}^{\beta 1} + \varepsilon_{1i} \quad (13)$$

$$BGB_i = \alpha_2 X_{2i}^{\beta 2} + \varepsilon_{2i} \quad (14)$$

$$TB_i = \alpha_1 X_{1i}^{\beta 1} + \varepsilon_{1i} + \alpha_2 X_{2i}^{\beta 2} + \varepsilon_{2i} \quad (15)$$

where AGB_i, BGB_i, and TB_i are the *AGB, BGB*, and *TB,* respectively, for the i^{th} sample tree; $\alpha_{1,2}$ and $\beta_{1,2}$ are parameters of the 1st, 2nd model; $X_{1,2i}$ is the predictor variable(s) including *DBH, H, WD* and *CA* or a combination of predictor variables associated with the i^{th} tree for the 1st, 2nd model; and $e_{1,2i}$ is the random error term associated with the i^{th} tree for the 1st, 2nd model and are assumed to be normally distributed with mean zero and constant variance.

Through implemented cross validation, we compared the errors and reliability of simultaneous predictions of tree *AGB, BGB* and *TB* in tropical forests by using MODL models against modeling systems applying WNSUR (Kralicek et al., 2017) with the same forest types of DF or EBLF, using the same sampled trees and for the same tree predictor covariates based on FI, Bias, RMSPE and MAPE of simultaneous predictions of tree *AGB, BGB, TB*. The models used four tree optimal predictors *DBH, H, WD* and *CA* in DF and three optimal predictors *DBH, H* and *WD* in EBLF. The results of the cross-validation comparisons are presented in Table 7. These comparisons are visually depicted in Fig. 5, showcasing the simultaneous fitting and observation of tree biomass components while comparing the two approaches. A significant outcome of this analysis is that the MODL approach improved reliability and accuracy compared to the WNSUR method for the simultaneous prediction of tree *AGB, BGB*, and the total biomass *TB* in tropical forests.

The MODL models in this study provided significantly better reliability than the WNSUR models of Kralicek et al. (2017) for simultaneous predictions of tree *AGB, BGB,* and *TB* in tropical forests (Table 7). For dipterocarp forests with the same predictive tree variables, the MODL models reduced the MAPE of simultaneous predictions of tree *AGB, BGB,* and *TB* by 15.7 %, 22.2 %, and 11.6 %, respectively, compared to the WNSUR modeling system (Table 7). For evergreen broadleaf forests, MODL models reduced the MAPE of simultaneous predictions of tree *AGB, BGB,* and *TB* by up to 24.7 %, 96.5 %, and 9.4 %,

Table 3
The best Multi-Output Deep Learning (MODL) models of different combinations of predictive variables for simultaneously predicting tree *AGB, BGB*, and *TB* while ensuring additivity in two forest types, DF and EBLF and cross-validation statistics.

ID	Combinations of predictive variables for simultaneously predicting tree *AGB, BGB* and *TB*	FI	RMSE (kg tree^{-1})	Bias (%)	RMSPE (%)	MAPE (%)
1	**8 predictive variables: *DBH, CA, H, WD, BA, Altitude, P, Forest type***					
	Predicting *AGB*:	0.875	16.6	−0.98	21.47	16.42
	Predicting *BGB*:	0.791	5.9	2.34	38.90	29.01
	Predicting *TB* = *AGB* + *BGB*:	0.922	12.5	2.08	19.03	14.90
2	7 predictive variables: *DBH, CA, H, WD, BA, Altitude, Forest type*					
	Predicting *AGB*:	0.856	42.7	−5.39	23.20	18.32
	Predicting *BGB*:	0.872	5.3	6.37	37.15	28.55
	Predicting *TB* = *AGB* + *BGB*:	0.881	30.4	−0.19	19.76	15.50
3	6 predictive variables: *DBH, CA, H, WD, BA, Forest type*					
	Predicting *AGB*:	0.898	24.5	−0.95	23.31	17.78
	Predicting *BGB*:	0.750	8.9	0.89	34.27	26.27
	Predicting *TB* = *AGB* + *BGB*:	0.906	18.4	2.09	20.83	15.99
4	5 predictive variables: *DBH, CA, H, WD, Forest type*					
	Predicting *AGB*:	0.920	13.8	−2.52	21.81	16.92
	Predicting *BGB*:	0.878	4.0	1.63	41.40	28.17
	Predicting *TB* = *AGB* + *BGB*:	0.938	10.1	2.00	17.69	14.21
5	4 predictive variables: *DBH, CA, H, Forest type*					
	Predicting *AGB*:	0.820	72.4	10.04	24.30	20.25
	Predicting *BGB*:	0.858	10.2	7.11	37.34	30.37
	Predicting *TB* = *AGB* + *BGB*:	0.841	51.7	12.04	24.33	20.95
6	4 predictive variables: *DBH, H, WD, Forest type*					
	Predicting *AGB*:	0.994	9.2	0.19	24.61	16.50
	Predicting *BGB*:	0.893	5.2	−4.10	43.32	31.08
	Predicting *TB* = *AGB* + *BGB*:	0.994	7.5	2.23	21.64	15.24
7	*3* predictive variables: *DBH, CA, Forest type*					
	Predicting *AGB*:	0.801	31.4	−4.14	33.14	23.99
	Predicting *BGB*:	0.703	6.0	11.28	33.84	26.96
	Predicting *TB* = *AGB* + *BGB*:	0.833	22.6	3.27	24.05	18.21
8	3 predictive variables: *DBH, H, Forest type*					
	Predicting *AGB*:	0.940	19.8	2.00	26.94	21.07
	Predicting *BGB*:	0.702	9.5	13.42	40.84	33.55
	Predicting *TB* = *AGB* + *BGB*:	0.929	15.5	5.97	27.02	21.17
9	*2* predictive variables: *DBH, Forest type*					
	Predicting *AGB*:	0.735	65.7	−0.14	32.07	24.06
	Predicting *BGB*:	0.882	5.7	10.71	30.31	24.15
	Predicting *TB* = *AGB* + *BGB*:	0.781	46.6	5.10	24.92	19.93

Note: *AGB* (kg tree^{-1}): Aboveground biomass, *BGB* (kg tree^{-1}): Belowground biomass, *TB* (kg tree^{-1}): Total tree biomass including tree above- and belowground biomass, *DBH* (cm): Diameter at breast height, *CA* (m^2 tree^{-1}): Tree crown area, *H* (m): Tree height, *WD* (g cm^{-3}): Wood density, *BA* (m^2/ha): Stand basal area, *Altitude* (m), *P* (mm year^{-1} averaged): Mean annual precipitation, *Forest type*: Dipterocarp Forest (DF) and Evergreen Broadleaf Forest (EBLF), *Soil type*: Igneous rocks and Sedimentary rocks.
Cross-validation with 10 realizations, each repeating the dataset was split randomly into 70% for training and 30% for validation; and the best MODL models, chosen from the 10 validation results, had its statistics and error metrics averaged for that validation. **Bold**: The optimal MODL model.

respectively, compared to the WNSUR modeling system (Table 7). These comparisons show a substantial improvement in reliability (especially for *AGB* and *BGB* predictions) when applying the MODL algorithm compared to the conventional method like WNSUR. These comparisons are further substantiated by Fig. 5.

Although the well-known WNSUR method offers interpretability, it is not without limitations, much like other regression-based approaches. For instance, it requires adherence to assumptions such as normality and homoscedasticity and necessitates the identification of optimal nonlinear fitting functions for each component equation. Furthermore, finding appropriate initial parameter estimates in the nonlinear modelling system can be challenging. The DL models can operate without the need for specific statistical assumptions, which makes them advantageous when dealing with the complexities and uncertainties present in tropical forest ecosystems.

4.2. Ecological and environmental variables in MODL models

Regression functions often fail to completely capture the environmental and ecological factors that impact the complex biological relationships involved in forest biomass and carbon sequestration in tropical forests (Huy et al., 2022). Previous research has focused on integrating key predictors specific to individual trees within biomass equations for tropical forests (Brown, 1997; Chave et al., 2014). As a result, these regression-based approaches frequently neglect the inclusion of other crucial factors that significantly impact the relationships between biomass and various environmental and ecological variables within tropical forests (Huy et al., 2022).

The MODL approach used in this study incorporates a comprehensive set of variables, including forest stand variables, ecological and environmental factors, and tree-level predictors. By considering a broader range of factors and variables, the MODL models capture the complex interactions and dependencies among these variables, resulting in more accurate and robust predictions for tree biomass in tropical forest ecosystems. Conventional regression techniques have the disadvantage of defining the functional forms of the relationship between the tree biomass component and the total biomass with these factors, primarily how to code nominal categorical variables and determine the optimal function to map these coded variables to tree biomass. Meanwhile, MODL models can incorporate such variables without knowledge of the relational function form. In MODL models, the categorical variables can be encoded by various techniques such as ordinal, one-hot, dummy, effect, hash, binary, base N, and target encodings (Huy et al., 2022) for the input layer of the DNNs. As a result, MODL models greatly improve the reliability of simultaneous predictions of tree components and total biomass.

In this study, the optimization of MODL for simultaneously predicting tree *AGB, BGB,* and *TB* while ensuring additivity included 8 predictive variables: *DBH, CA, H, WD, BA, Altitude, P,* and *Forest type*. The functional forms of the tree component and total biomass, along with ecological environmental factors such as *Altitude, P,* and *Forest type*, are complicated. Therefore, until now, most models simultaneously estimate tree components and total biomass with mainly tree predictors such as *DBH, H, WD,* and *CA* (Kralicek et al., 2017; Huy et al., 2019). Additionally, the sequestration of *AGB*, for example, is significantly influenced by variations in altitude gradients within Amazonian forests (Maza et al., 2022). Thanks to the inclusion of various input factors, the MODL models can be more widely applied to simulate complex biological, biometric, and ecological processes of tropical forests for sustainable management.

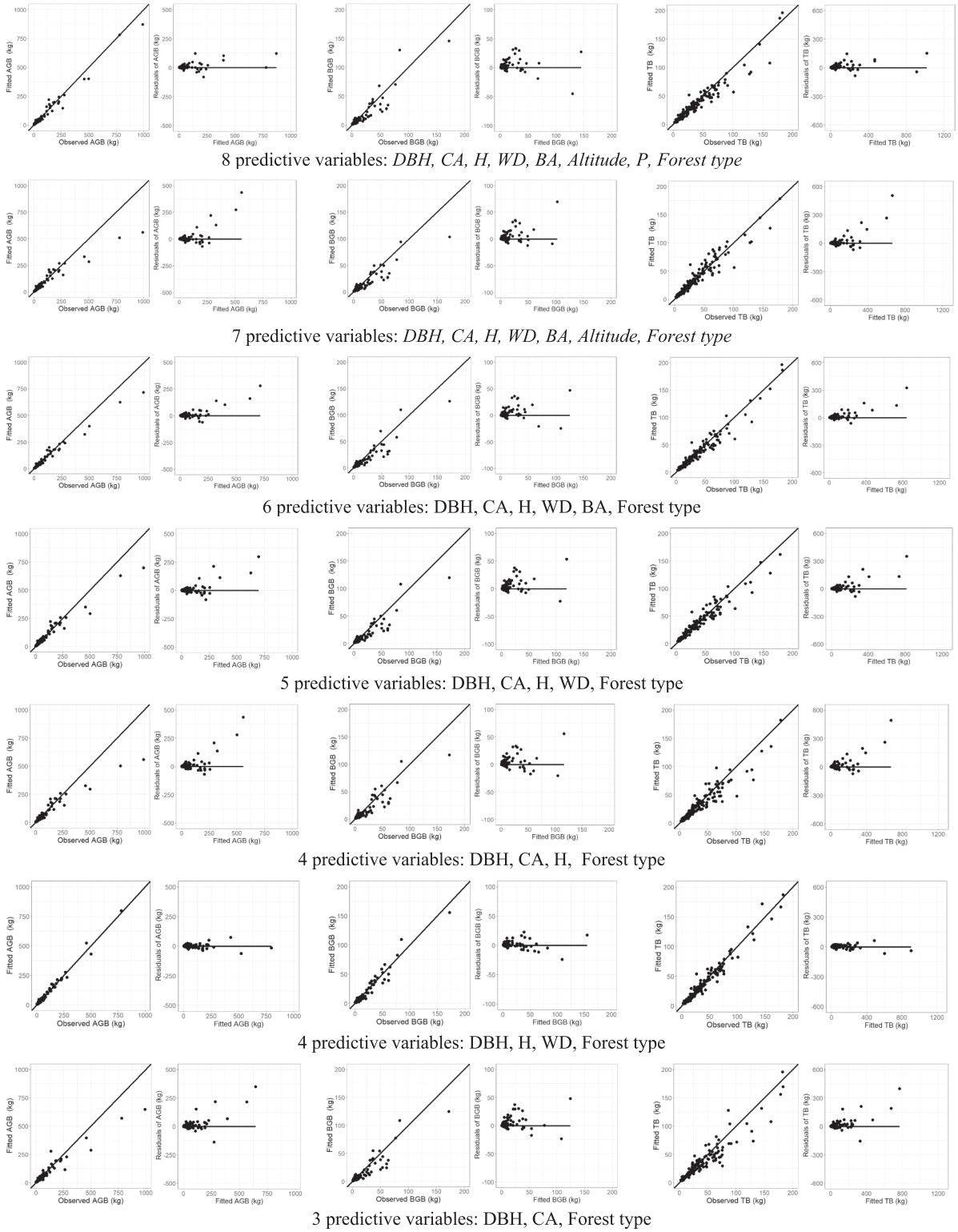

Fig. 4. Plots of Multi-Output Deep Learning (MODL) models for simultaneously fitting tree *AGB, BGB*, *TB* (tree above- and belowground biomass and the total tree biomass, respectively) associated with different combinations of predictive covariates: Fitted vs. Observed tree *AGB, BGB, TB* (left); Residuals of tree *AGB, BGB, TB* vs. Fitted tree *AGB, BGB, TB* (right). *DBH*: Diameter at breast height, *CA*: Tree crown area, *H*: Tree height, *WD*: Wood density, *BA*: Stand basal area, *Altitude*, *P*: Mean annual precipitation, *Forest type*: Dipterocarp Forest (DF) and Evergreen Broadleaf Forest (EBLF), *Soil type*: Igneous rocks and Sedimentary rocks.

4.3. Application of MODL models in tropical forests

Based on resource availability and the principle of parsimony, selecting and utilizing one of the 9 best-created MODL models presented in Table 3 is possible. The selected MODL model can then be applied to gather the necessary predictive covariates and assess their variations

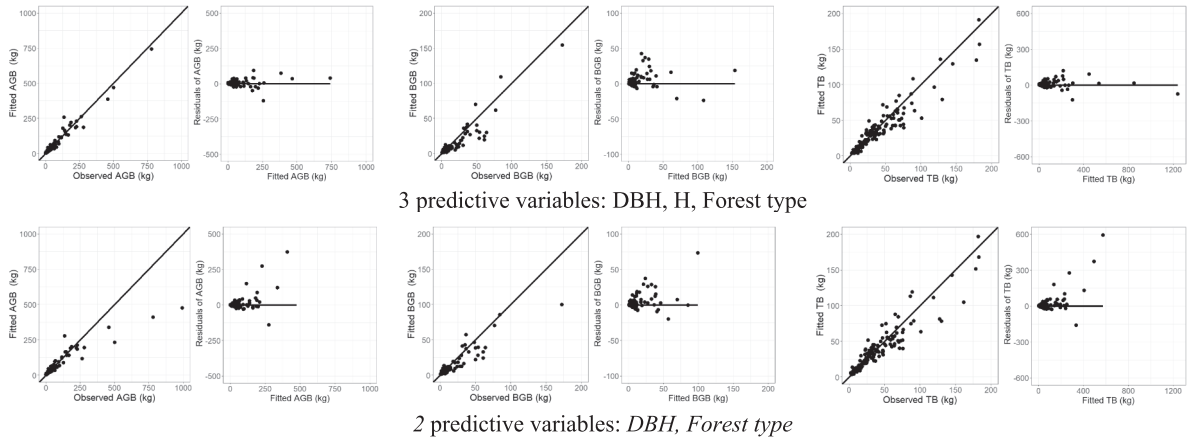

Fig. 4. (*continued*).

within the application region. The MODL model that incorporates eight predictive covariates *DBH, CA, H, WD, BA, Altitude, P,* and *Forest type* demonstrated the highest reliability for the simultaneous predictions of tree *AGB, BGB* and *TB* in both tropical forests DFs and EBLFs (Table 3). Following the identification of the eight optimal predictive MODL model, the MODL model featuring four predictive variables – *DBH, H, WD*, and *Forest type* (Table 3) – demonstrates a commendable goodness of fit for simultaneous prediction of *AGB, BGB*, and *TB*. This model warrants selection when applied within an ecological setting characterized by relatively stable variables, provided it adheres to the parsimony criteria. Additionally, when using MODL models for distinct forest types, utilizing the optimal MODL models (Table 4 and Table 5) tailored to the specific forest type yields superior results compared to using the MODL models across both forest types, as cross-validated in the cases of DFs and EBLFs (Table 4 and Table 5 vs. Table 3).

The application of the selected MODL model requires input observed data and can be applied to either a forest block or a larger region. To implement the model, new data for the predictor variables need to be collected based on the requirements of the chosen model. This can be achieved by collecting data from several purposive sample plots if the model is applied to a forest block or by establishing a systematic sampling design for a larger area. This study developed a Python script to load the saved best MODL model and apply it to the newly observed data. This script allows for simultaneous *AGB, BGB*, and *TB* predictions while ensuring additivity for each tree within the sample plot in both tropical forests, DFs, and EBLFs. From the results obtained, predicting and monitoring the total above- and below-ground biomass of forest trees for each forest block or a larger ecological region is possible. This capability allows for assessing changes in tree biomass over time and provides valuable information on the quantity and carbon storage within forest ecosystems.

The MODL models developed in this study are utilized for simultaneous predictions of *AGB, BGB*, and *TB* while maintaining additivity for individual forest trees and aggregated plot-level totals. These models can be extended for forest biomass estimation at larger scales through integration with remote sensing (RS) technology. MODL or conventional tree biomass models assist in providing ground truth data for total *AGB, BGB*, and *TB* per plot (Zhang et al., 2021), combined with various RS imagery analysis techniques to establish relationships between forest biomass and image indices. This enables prediction of total *AGB, BGB*, and *TB* across wide areas for different forest statuses and types. However, RS imagery, with its variable resolutions, cannot directly capture *AGB, BGB*, and *TB* values in tropical forests (Zhang et al., 2021), which are obtained only through destructive sampling methods. Conventional tree biomass regression and MODL methods utilize these destructive sampling data to develop tree biomass models, incorporating predictors such as tree/stand-level variables and ecological/environmental factors. MODL models or biomass allometric equations then transfer predictors from tree/stand-levels and ecological/environmental factors to estimate forest stand biomass, supporting RS analysis in large-scale forest biomass prediction. High-resolution multispectral images obtained from Unmanned Aerial Vehicles (UAVs) and Light Detection and Ranging (LiDAR) technology can be used to develop prediction models, both parametric and non-parametric, for estimating annual crop plant biomass based on spectral indices (Liu et al., 2022, 2023, 2024; Lao et al., 2024). Nevertheless, in tropical rainforests, UAVs, LiDAR can only capture tree variables and stand attributes, such as tree *H*, tree *CD*, and stand *N* (Terryn et al., 2022). Thus, conventional tree biomass regression or MODL models, as recommended in this study, are necessary to translate tree/stand attributes obtained via UAVs into forest biomass estimates (Zhang et al., 2021).

4.4. Novelty of the MODL models developed in this study

While DL models outperform conventional regression methods in biometrics research within tropical forests, as demonstrated by studies (Ogana and Ercanli, 2021; Huy et al., 2022; Qin et al., 2023), existing DL models only focused on predicting individual factors like tree *H*, tree crown width, and tree *AGB*. This study introduced a novel approach for simultaneous prediction of *AGB* and *BGB* using MODL method. This study's key innovations included designing an optimal architecture for DNN to tailor MODL models to tropical forest biomass data, which often contain diverse influencing factors. Additionally, for the first time, an algorithm was designed to address the specific loss function tailored for creating MODL models that predict *AGB, BGB*, and *TB* simultaneously, while ensuring additivity ($TB = AGB + BGB$). The constructed MODL models demonstrated superior reliability compared to conventional regression modeling systems, which also predict simultaneous components of forest tree biomass and ensure additivity like WNSUR. A distinguishing feature in the construction of MODL, as opposed to conventional correlational models relying solely on tree-level predictors to estimate forest tree biomass, MODL has been designed to incorporate a diverse array of selected predictors influencing forest tree biomass, such as tree-level variables, stand-level factors, environmental, and ecological variables identified using the FAMD method, wherein complex numerical and categorical variables are incorporated to enhance reliability and applicability scope. The results indicated that among the MODL models created, the model utilizing the optimal eight predictors: *DBH, CA, H, WD, BA, Altitude, P*, and *Forest type* performed the best. This optimal MODL model can be applied across various scales, from small forest plots to large landscapes, due to its inclusion of diverse predictors and coverage of their gradients, enhancing its flexibility and applicability.

Despite the advancements in DL techniques across various fields, the

Table 4
The best Multi-Output Deep Learning (MODL) models of different combinations of predictive variables for simultaneously predicting tree *AGB, BGB,* and *TB* while ensuring additivity for dipterocarp forest (DF) and cross-validation statistics.

ID	Combinations of predictive variables for simultaneously predicting tree *AGB, BGB* and *TB*	FI	RMSE (kg tree^{-1})	Bias (%)	RMSPE (%)	MAPE (%)
1	6 predictive variables: *DBH, CA, H, WD, BA, Altitude*					
	Predicting *AGB*:	0.947	40.4	3.00	23.14	19.72
	Predicting *BGB*:	0.892	10.5	11.51	26.95	21.28
	Predicting *TB* = *AGB* + *BGB*:	0.944	29.5	6.41	20.77	17.47
2	5 predictive variables: *DBH, CA, H, WD, BA*					
	Predicting *AGB*:	0.915	49.8	−0.51	23.01	18.85
	Predicting *BGB*:	0.906	9.1	14.60	26.18	22.39
	Predicting *TB* = *AGB* + *BGB*:	0.915	35.8	3.68	19.93	16.19
3	**4 predictive variables: *DBH, CA, H, WD***					
	Predicting *AGB*:	0.981	9.2	−3.33	17.68	13.22
	Predicting *BGB*:	0.719	8.8	6.31	38.22	27.72
	Predicting *TB* = *AGB* + *BGB*:	0.965	9.0	2.05	13.85	10.95
4	3 predictive variables: *DBH, CA, H*					
	Predicting *AGB*:	0.945	21.7	−2.29	26.01	21.40
	Predicting *BGB*:	0.871	6.1	13.96	29.16	21.98
	Predicting *TB* = *AGB* + *BGB*:	0.944	15.9	3.05	22.20	18.46
5	3 predictive variables: *DBH, H, WD*					
	Predicting *AGB*:	0.741	89.5	−4.82	28.00	19.83
	Predicting *BGB*:	0.804	14.1	6.94	29.36	23.93
	Predicting *TB* = *AGB* + *BGB*:	0.755	64.1	0.73	21.34	14.06
6	2 predictive variables: *DBH, CA*					
	Predicting *AGB*:	0.950	15.8	0.21	24.75	20.03
	Predicting *BGB*:	0.732	8.4	10.86	34.16	25.46
	Predicting *TB* = *AGB* + *BGB*:	0.924	12.7	5.41	22.54	17.83
7	2 predictive variables: *DBH, H*					
	Predicting *AGB*:	0.934	12.5	6.21	25.03	19.49
	Predicting *BGB*:	0.643	8.4	9.22	45.34	33.94
	Predicting *TB* = *AGB* + *BGB*:	0.907	10.6	10.06	23.41	18.44
8	1 predictive variable: *DBH*					
	Predicting *AGB*:	0.954	13.9	−0.16	23.79	20.22
	Predicting *BGB*:	0.827	6.5	2.74	41.64	27.99
	Predicting *TB* = *AGB* + *BGB*:	0.950	10.8	4.77	20.78	17.33

Note: *AGB* (kg tree^{-1}): Aboveground biomass, *BGB* (kg tree^{-1}): Belowground biomass, *TB* (kg tree^{-1}): Total tree biomass including tree above- and belowground biomass, *DBH* (cm): Diameter at breast height, *CA* (m^2 tree^{-1}): Tree crown area, *H* (m): Tree height, *WD* (g cm^{-3}): Wood density, *BA* (m^2/ha): Stand basal area, *Altitude* (m), *P* (mm year^{-1} averaged): Mean annual precipitation, *Soil type*: Igneous rocks and Sedimentary rocks.
Cross-validation with 10 realizations, each repeating the dataset was split randomly into 70% for training and 30% for validation; and the best MODL models, chosen from the 10 validation results, had its statistics and error metrics averaged for that validation. **Bold**: The optimal MODL model.

MODL model as developed in this study is novel and has not been found through literature review. The new methodology introduced in this study will enable the exploration of intricate connections within tropical forest ecosystems, which encompass multiple predictors and responses

Table 5
The best Multi-Output Deep Learning (MODL) models of different combinations of predictive variables for simultaneously predicting tree *AGB, BGB,* and *TB* while ensuring additivity for evergreen broadleaf forest (EBLF) and cross-validation statistics.

ID	Combinations of predictive variables for simultaneously predicting tree *AGB, BGB* and *TB*	FI	RMSE (kg tree^{-1})	Bias (%)	RMSPE (%)	MAPE (%)
1	7 predictive variables: *DBH, CA, H, WD, BA, Altitude, P*					
	Predicting *AGB*:	0.891	7.4	0.91	16.69	12.68
	Predicting *BGB*:	0.741	2.8	2.18	46.07	27.91
	Predicting *TB* = *AGB* + *BGB*:	0.891	5.6	2.44	17.25	12.34
2	6 predictive variables: *DBH, CA, H, WD, BA, Altitude*					
	Predicting *AGB*:	0.934	7.2	−1.72	19.94	15.84
	Predicting *BGB*:	0.805	3.0	6.22	28.26	20.99
	Predicting *TB* = *AGB* + *BGB*:	0.925	5.5	0.60	17.94	14.42
3	5 predictive variables: *DBH, CA, H, WD, BA*					
	Predicting *AGB*:	0.855	8.6	−0.47	32.81	16.29
	Predicting *BGB*:	0.793	2.8	5.87	24.90	21.19
	Predicting *TB* = *AGB* + *BGB*:	0.896	6.4	2.54	23.40	13.66
4	4 predictive variables: *DBH, CA, H, WD*					
	Predicting *AGB*:	0.661	59.4	7.19	19.68	14.71
	Predicting *BGB*:	0.745	7.6	8.22	28.37	25.09
	Predicting *TB* = *AGB* + *BGB*:	0.737	42.4	8.77	19.06	14.38
5	3 predictive variables: *DBH, CA, H*					
	Predicting *AGB*:	0.826	11.3	5.25	17.43	13.87
	Predicting *BGB*:	0.472	5.0	16.41	35.66	30.94
	Predicting *TB* = *AGB* + *BGB*:	0.776	8.7	8.06	18.34	13.69
6	**3 predictive variables: *DBH, H, WD***					
	Predicting *AGB*:	0.884	9.8	1.70	15.26	12.44
	Predicting *BGB*:	0.684	7.4	10.72	30.58	25.60
	Predicting *TB* = *AGB* + *BGB*:	0.947	8.7	4.76	14.15	10.56
7	2 predictive variables: *DBH, CA*					
	Predicting *AGB*:	0.555	68.0	9.39	25.90	20.32
	Predicting *BGB*:	0.905	3.0	6.03	39.39	26.84
	Predicting *TB* = *AGB* + *BGB*:	0.599	48.1	9.73	26.29	20.60
8	2 predictive variables: *DBH, H*					
	Predicting *AGB*:	0.821	44.1	6.37	22.50	17.28
	Predicting *BGB*:	0.899	3.6	8.76	31.60	26.59
	Predicting *TB* = *AGB* + *BGB*:	0.865	31.3	7.82	21.71	16.43
9	1 predictive variable: *DBH*					
	Predicting *AGB*:	0.829	11.0	9.25	23.67	18.05
	Predicting *BGB*:	0.676	3.8	7.16	27.09	21.78
	Predicting *TB* = *AGB* + *BGB*:	0.816	8.3	9.83	22.66	16.55

Note: *AGB* (kg tree^{-1}): Aboveground biomass, *BGB* (kg tree^{-1}): Belowground biomass, *TB* (kg tree^{-1}): Total tree biomass including tree above- and belowground biomass, *DBH* (cm): Diameter at breast height, *CA* (m^2 tree^{-1}): Tree crown area, *H* (m): Tree height, *WD* (g cm^{-3}): Wood density, *BA* (m^2/ha): Stand basal area, *Altitude* (m), *P* (mm year^{-1} averaged): Mean annual precipitation, *Soil type*: Igneous rocks and Sedimentary rocks.
Cross-validation with 10 realizations, each repeating the dataset was split randomly into 70% for training and 30% for validation; and the best MODL models, chosen from the 10 validation results, had its statistics and error metrics averaged for that validation. **Bold**: The optimal MODL model.

Table 6
The best Single-Output Deep Learning models with different combinations of 8 optimal variables and a minimum of 2 variables for separately predicting tree *AGB, BGB, TB* in two forest types, DF and EBLF, and cross-validation statistics.

ID	Combinations of predictive variables	Separately predicted tree *AGB, BGB,* and *TB*	FI	RMSE (kg tree^{-1})	Bias (%)	RMSPE (%)	MAPE (%)
1	8 predictive variables: *DBH, CA, H, WD, BA, Altitude, P, Forest type*	Predicting *AGB:*	0.929	39.8	3.29	20.14	15.08
		Predicting *BGB:*	0.853	10.0	2.95	27.35	22.07
		Predicting *TB:*	0.983	25.9	1.33	25.96	17.59
2	2 predictive variables: *DBH, Forest type*	Predicting *AGB:*	0.944	29.1	2.62	26.62	22.22
		Predicting *BGB:*	0.896	3.9	5.44	34.21	28.13
		Predicting *TB:*	0.970	28.6	7.40	24.38	17.92

Note: *AGB* (kg tree^{-1}): Aboveground biomass, *BGB* (kg tree^{-1}): Belowground biomass, *TB* (kg tree^{-1}): Total tree biomass including tree above- and belowground biomass, *DBH* (cm): Diameter at breast height, *CA* (m^2 tree^{-1}): Tree crown area, *H* (m): Tree height, *WD* (g cm^{-3}): Wood density, *BA* (m^2/ha): Stand basal area, *Altitude* (m), *P* (mm year^{-1} averaged): Mean annual precipitation, *Forest type*: Dipterocarp Forest (DF) and Evergreen Broadleaf Forest (EBLF), *Soil type*: Igneous rocks and Sedimentary rocks.Cross-validation with 10 realizations, each repeating the dataset was split randomly into 70 % for training and 30 % for validation; and the best MODL models, chosen from the 10 validation results, had its statistics and error metrics averaged for that validation.

Table 7
Cross-validation statistics and error metrics comparing Multi-Output Deep Learning (MODL) and Weighted Nonlinear Seemingly Unrelated Regression (WNSUR) models for simultaneous predictions of tree *AGB, BGB,* and *TB* while ensuring additivity in each forest type of DF and EBLF, using the same sampled trees, and tree predictive covariates.

ID	Tree predictive covariates	Forest types / sampled trees (n)	Methods	Modelling systems	FI	Bias (%)	RMSPE (%)	MAPE (%)	Sources
1	*DBH, H, WD, CA*	DF n = 105	WNSUR	$AGB = 0.79787 \times (DBH^2HWD)^{0.66765} \times CA^{0.51024}$	0.956	−0.38	35.21	28.92	Kralicek et al., 2017
				$BGB = 56.47582 \times (DBH^2H)^{0.91319}$	0.885	−15.24	69.81	49.94	
				$TB = AGB + BGB$	0.949	0.15	27.49	22.54	
			MODL	*The best model for predicting AGB*	0.981	−3.33	17.68	13.22	This study, 2023
				The best model for predicting BGB	0.719	6.31	38.22	27.72	
				The best model for predicting $TB = AGB + BGB$	0.965	2.05	13.85	10.95	
2	*DBH, H, WD*	EBLF n = 70	WNSUR	$AGB = 0.14822 \times (DBH^2HWD)^{1.23945}$	0.889	27.68	42.99	37.09	Kralicek et al., 2017
				$BGB = 0.16892 \times DBH^{1.76536}$	0.769	−111.14	158.26	122.14	
				$TB = AGB + BGB$	0.909	9.97	25.58	19.92	
			MODL	*The best model for predicting AGB*	0.884	1.70	15.26	12.44	This study, 2023
				The best model for predicting BGB	0.684	10.72	30.58	25.60	
				The best model for predicting $TB = AGB + BGB$	0.947	4.76	14.15	10.56	

Note: *AGB* (kg tree^{-1}): Aboveground biomass, *BGB* (kg tree^{-1}): Belowground biomass, *TB* (kg tree^{-1}): Total tree biomass including tree above- and belowground biomass, *DBH* (cm): Diameter at breast height, *CA* (m^2 tree^{-1}): Tree crown area, *H* (m): Tree height, *WD* (g cm^{-3}): Wood density. Cross-validation for MODL with 10 realizations, each repeating the dataset, was split randomly into 70 % for training and 30 % for validation; the best MODL model was selected out of 10 validation results, and had its statistics and error metrics averaged for that validation. DBH^2H (m^3)= (*DBH* (cm)/100)^2 × *H* (m); DBH^2HWD (kg) = DBH^2H × WD (g cm^{-3}) × 1000. DF: Dipterocarp Forest, EBLF: Evergreen Broadleaf Forest. The WNSUR modeling systems exhibited all parameters as significant at a p-value < 0.0001.

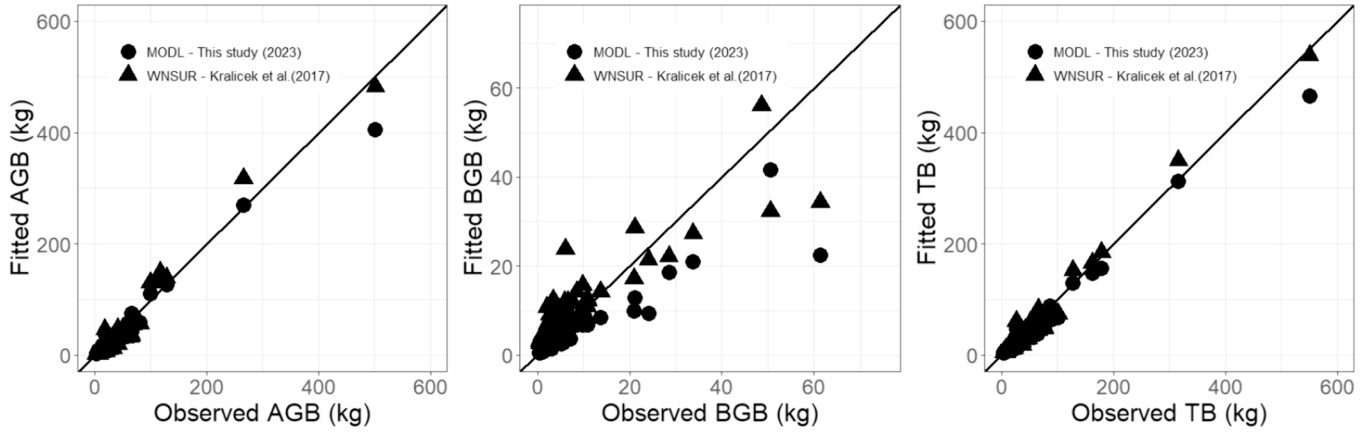

Fig. 5. Simultaneously fitted vs. observed tree *AGB, BGB*, and *TB* (tree above- and belowground biomass and the total tree biomass, respectively) with the same tree predictors of *DBH, H,* and *WD* (diameter at breast height, tree height, and wood density, respectively) for evergreen broadleaf forests in comparison between Multi-Output Deep Learning (MODL) and Weighted Nonlinear Seemingly Unrelated Regression (WNSUR) approaches.

intertwined in biological and ecological contexts. These relationships are challenging to capture with conventional regression models.

4.5. Limitations of the MODL approach

In addition to the advantages of MODL models over conventional regression WNSUR in simultaneous forest biomass prediction and ensuring additivity, they have limitations: 1) They require large datasets for accurate learning of multi-predictor-multi-output relationships; 2) MODL lacks a mechanism for selecting influential predictor variables, necessitating reliance on methods like PCA, FAMD for selection; and 3) Optimization of DNN architecture for each dataset entails exploring various factors, making training time-consuming.

5. Conclusions

The MODL modeling systems developed in this study significantly increased the reliability of simultaneous predictions of tree *AGB, BGB,* and *TB* in DF and EBLF compared to conventional WNSUR modeling systems, even when both utilized the same dataset and predictive covariates in the same forest types. Additionally, they ensured the additivity of the tree components and total biomass estimates, a feat impossible through single-output DL models used for separate predictions. The MODL models reduced the MAPE of tree *AGB, BGB,* and *TB* simultaneous predictions by up to 24.7 %, 96.5 %, and 9.4 %, respectively, compared to WNSUR modeling systems.

The MODL models with one to eight input predictors were developed and saved. The MODL model with the optimal eight predictive covariates – *DBH, CA, H, WD, BA, Altitude, P, and Forest type* – proved the best for simultaneous tree *AGB, BGB,* and *TB* predictions in tropical DFs and EBLFs. The MODL algorithm can incorporate many complex factors, including numerical and categorical variables, into the models without needing pre-identifying optimal functions. This characteristic significantly enhances the reliability of simultaneous predictions for tree *AGB, BGB*, and *TB*. It enables the MODL models to be applied across various scales, spanning from small to large areas, encompassing diverse gradients of forest stand characteristics, climate conditions, soil properties, and topography.

Funding

The dataset was collected and compiled as part of the vital research funded by the Ministry of Education and Training of Vietnam under code B2010-15-33TD.

CRediT authorship contribution statement

Bao Huy: Writing – review & editing, Writing – original draft, Visualization, Validation, Software, Resources, Methodology, Investigation, Funding acquisition, Formal analysis, Data curation, Conceptualization. **Nguyen Quy Truong:** Writing – original draft, Visualization, Validation, Software, Methodology, Formal analysis, Data curation, Conceptualization. **Krishna P. Poudel:** Writing – review & editing, Validation, Methodology. **Hailemariam Temesgen:** Writing – review & editing, Validation, Supervision, Methodology. **Nguyen Quy Khiem:** Writing – original draft, Project administration, Investigation, Formal analysis, Data curation.

Declaration of competing interest

The authors declare that they have no known competing financial interests or personal relationships that could have appeared to influence the work reported in this paper.

Data availability

Data will be made available on request.

Acknowledgments

Thanks to the Forest Resources and Environment Management (FREM) field team for their tremendous efforts in collecting the region's largest databases of the tree above – belowground biomass.

References

Affleck, D.L.R., Dieguez-Aranda, U., 2016. Additive nonlinear biomass equations: a likelihood-based approach. For. Sci. 62 (2), 129–140.

Alzubaidi, L., Zhang, J., Humaidi, A.J., Dujaili, A.A., Duan, Y., Al-Shamma, O., Santamaría, J., Fadhel, Al-Amidie, M., Farhan, L., 2021. Review of deep learning: concepts, CNN architectures, challenges, applications, future directions. J. Big Data (2021) 8:53. DOI: 10.1186/s40537-021-00444-8.

Brahma, B., Nath, A.J., Deb, C., Sileshi, G.W., Sahoo, U.K., Das, A.K., 2021. A critical review of forest biomass estimation equations in India. Trees Forests People 5 (2021), 100098. https://doi.org/10.1016/j.tfp.2021.100098.

Chave, J., Mechain, M.R., Burquez, A., Chidumayo, E., Colgan, M.S., Delitti, W.B.C., Duque, A., Eid, T., Fearnside, P.M., Goodman, R.C., Henry, M., Yrizar, A.M., Mugasha, W.A., Mullerlandau, H.C., Mencuccini, M., Nelson, B.W., Ngomanda, A., Nogueira, E.M., Ortiz-Malavassi, E., Pelissier, R., Ploton, P., Ryan, C.M., Saldarriaga, J.G., Vieilledent, G., 2014. Improved allometric models to estimate the aboveground biomass of tropical trees. Glob. Chang. Biol. 20 (2014), 3177–3190. https://doi.org/10.1111/gcb.12629.

Chollet, F., 2018. Deep Learning with Python. Manning, Shelter Island, NY, USA, 386 pp.

Christin, S., Hervet, E., Lecomte, N., 2019. Applications for deep learning in ecology. Methods Ecol. Evol. 2019 (10), 1632–1644. https://doi.org/10.1111/2041-210X.13256.

FAO, Guidelines for Country Reporting to FRA 2010. Working Paper 143, FAO, Rome, 2008, 80 pp.

Fick, S.E., Hijmans, R.J., 2017. WorldClim 2: new 1km spatial resolution climate surfaces for global land areas. Int. J. Climatol. 37 (12), 4302–4315.

Fischer, G., Nachtergaele, F.O., Prieler, S., Teixeira, E., Toth, G., van Velthuizen, H., Verelst, L., Wiberg, D., 2008. Global Agro-ecological Zones Assessment for Agriculture (GAEZ 2008). IIASA, Laxenburg, Austria and FAO, Rome, Italy.

Güner, S.T., Diamantopoulou, M.J., Poudel, K.P., Comez, A., Ozcelik, R., 2022. Employing artificial neural network for effective biomass prediction: An alternative approach. Comput. Electron. Agric. 192 (2022), 106596.

Hoover, K., Riddle, A.A., 2020. Forest Carbon Primer. Congressional Research Service (CRS), pp. 30. Available at https://sgp.fas.org/crs/misc/R46312.pd, accessed 29 May 2023.

Huy, B., Poudel, K.P., Kralicek, K., Hung, N.D., Khoa, P.V., Phuong, V.T., Temesgen, H., 2016b. Allometric equations for estimating tree aboveground biomass in tropical dipterocarp forests of Viet Nam. Forests 2016, 7(180): 1-19. DOI: 10.3390/f7080180, http://www.mdpi.com/1999-4907/7/8/180.

Huy, B., Truong, N.Q., Khiem, N.Q., Poudel, K.P., Temesgen, H., 2022. Deep learning models for improved reliability of tree aboveground biomass prediction in the tropical evergreen broadleaf forests. For. Ecol. Manage. 508 (2022) 120031: 1-13. DOI: 10.1016/j.foreco.2022.120031.

Huy, B., Kralicek, K., Poudel, K.P., Phương, V.T., Khoa, P.V., Hung, N.D., Temesgen, H., 2016a. Allometric equations for estimating tree aboveground biomass in evergreen broadleaf forests of Viet Nam. For. Ecol. Manage. 382 (2016), 193–205. https://doi.org/10.1016/j.foreco.2016.10.021.

Huy, B., Tinh, N.T., Poudel, K.P., Frank, B.M., Temesgen, H., 2019. Taxon-specific modeling systems for improving reliability of tree aboveground biomass and its components estimates in tropical dry dipterocarp forests. For. Ecol. Manage. 437 (2019), 156–174.

IPCC, 2006. IPCC Guidelines for National Greenhouse Gas Inventories. Prepared by the National Greenhouse Gas Inventories Programme, Eggleston H.S., Buendia L., Miwa K., Ngara T., Tanabe K., (eds). Published: IGES, Japan.

Kachamba, D.J., Eid, T., Gobakken, T., 2016. Above- and Below-ground Biomass Models for Trees in the Miombo Woodlands of Malawi. Forests 2016, 7, 38; doi:10.3390/f7020038.

Kenzo, T., Ichie, T., Hattori, D., Itioka, T., Handa, C., Ohkubo, T., Kendawang, J.J., Nakamura, M., Sakaguchi, M., Takahashi, N., Okamoto, M., Tanaka-Oda, A., Sakurai, K., Ninomiya, I., 2009. Development of allometric relationships for accurate estimation of above- and below-ground biomass in tropical secondary forests in Sarawak, Malaysia. J. Trop. Ecol. 25 (4), 371–386. https://doi.org/10.1017/S0266467409006129.

Keras, 2022. K Keras – Simple. Flexible. Powerful. https://keras.io/.

Koala, J., Sawadogo, L., Savadogo, P., Aynekulu, E., Heiskanen, J., Said, M., 2017. Allometric equations for below-ground biomass of four key woody species in West African savanna-woodlands. Silva Fennica vol. 51 no. 3 article id 1631. 15 p. DOI: 10.14214/sf.1631.

Kralicek, K., Huy, B., Poudel, K.P., Temesgen, H., Salas, C., 2017. Simultaneous estimation of above- and below-ground biomass in tropical forests of Vietnam. For. Ecol. Manage. 390 (2017), 147–156. http://www.sciencedirect.com/science/article/pii/S0378112716307411.

Lao, Z., Fu, B., Wei, Y., Deng, T., He, W., Yang, Y., He, H., Gao, E., 2024. Retrieval of chlorophyll content for vegetation communities under different inundation frequencies using UAV images and field measurements. Ecol. Ind. 158 (2024), 11132. https://doi.org/10.1016/j.ecolind.2023.111329.

LeCun, Y., Bengio, Y., Hinton, G., 2015. Deep learning. Nature 521 (2015), 436–444. https://doi.org/10.1038/nature14539.

Liu, Y., Feng, H., Yue, J., Li, Z., Yang, G., Song, X., Yang, X., Zhao, Y., 2022. Remote-sensing estimation of potato above-ground biomass based on spectral and spatial features extracted from high-definition digital camera images. Comput. Electron. Agric. 198 (2022), 107089 https://doi.org/10.1016/j.compag.2022.107089.

Liu, Y., Feng, H., Yue, J., Fan, Y., Bian, M., Ma, Y., Jin, X., Song, X., Yang, G., Zhao, Y., 2023. Estimating potato above-ground biomass by using integrated unmanned aerial system-based optical, structural, and textural canopy measurements. Comput. Electron. Agric. 213 (2023), 108229 https://doi.org/10.1016/j.compag.2023.108229.

Liu, Y., Feng, H., Fan, Y., Yue, J., Chen, R., Ma, Y., Bian, M., Yang, G., 2024. Improving potato above ground biomass estimation combining hyperspectral data and harmonic decomposition techniques. Comput. Electron. Agric. 318 (2024), 108699 https://doi.org/10.1016/j.compag.2024.108699.

Magalhaes, T.M., 2015. Allometric equations for estimating below-ground biomass of *Androstachys johnsonii* Prain. Carbon Balance Manage (2015): 10:16. DOI 10.1186/s13021-015-0027-4.

Marziliano, P.A., Lafortezza, R., Medicamento, U., Lorusso, L., Giannico, V., Colangelo, G., Sanesi, G., 2015. Estimating below-ground biomass and root/shoot ratio of *Phillyrea latifolia* L. in the Mediterranean forest landscapes. Annals Forest Sci. (2015) 72: 585-593 DOI10.1007/s13595-015-0486-5.

Maza, B., Rodes-Blanco, M., Rojas, E., 2022. Aboveground biomass along an elevation gradient in an evergreen Andean-Amazonian forest in Ecuador. Front. Glob. Change 5–2022. https://doi.org/10.3389/ffgc.2022.738585.

Medrano-Meraz, F., Lopez-Lopez, M.A., Angeles-Perez, G., Cruz-Cobos, F., Jozeph-de-Jong, B.H., 2021. Allometric equations for belowground biomass and carbon content of *Pinus patula* Schl. et Cham. Rev. Fitotec. Mex. Vol. 44 (3), 443–454.

Nair, V., Hinton, G.E., 2010. Rectified linear units improve restricted boltzmann machines. In: Proceedings of the 27th International Conference on International Conference on Machine Learning, Haifa, Israel, 2010, pp. 807–814.

Newell, J.P., Vos, R.O., 2012. Accounting for forest carbon pool dynamics in product carbon footprints: challenges and opportunities. Environ. Impact Assess. Rev. 37 (2012), 23–36.

Ogana, F.N., Ercanli, I., 2021. Modelling height-diameter relationships in complex tropical rain forest ecosystems using deep learning algorithm. J. For. Res. https://doi.org/10.1007/s11676-021-01373-1.

Parresol, B.R., 2001. Additivity of nonlinear biomass equations. Can. J. For. Res. 31 (5), 865–878.

Pelletier, J., Codjia, C., Potvin, C., 2012. Traditional shifting agriculture: tracking forest carbon stock and biodiversity through time in western Panama. Glob. Chang. Biol. 2012 (18), 3581–3595. https://doi.org/10.1111/j.1365-2486.2012.02788.x.

Poudel, K.P., Temesgen, H., 2016. Methods for estimating aboveground biomass and its components for Douglas-fir and lodgepole pine trees. Can. J. For. Res. 46: 77–87; dx.doi.org/10.1139/cjfr-2015-0256.

Python (2022). Python Packaging User Guide. https://packaging.python.org/.

Qin, Y., Wu, B., Lei, X., Feng, L., 2023. Prediction of tree crown width in natural mixed forests using deep learning algorithm, Forest Ecosystems (2023), doi DOI: 10.1016/j.fecs.2023.100109.

R Core Team, 2023. A language and environment for statistical computing. R Foundation for Statistical Computing, Vienna, Austria. http://www.r-project.org/index.html.

Razakamanarivo, R.H., Razakavololona, A., Razafindrakoto, M.A., Vieilledent, G., Albrecht, A., 2012. Below-ground biomass production and allometric relationships of eucalyptus coppice plantation in the central highlands of Madagascar. Biomass Bioenergy 45 (2012), 1–10.

Röhling, S., Demant, B., Dunger, K., Neubauer, M., Oehmichen, K., Riedel, T., Stümer, W., 2019. Equations for estimating belowground biomass of Silver Birch, Oak and Scots Pine in Germany. iForest 12: 166-172. – doi: 10.3832/ifor2862-012 [online 2019-03-15].

Sanquetta, C.R., Behling, A., Corte, A.P.D., Netto, S.P., Schikowski, A.B., 2015. Simultaneous estimation as alternative to independent modeling of tree biomass. Ann. For. Sci. 72 (8), 1099–1112.

SAS Institute Inc., 2014. SAS/ETS® 13.2 User's Guide. Chapter 19: The MODEL Procedure. Cary, NC: SAS Institute Inc. pp. 1067-1373.

Seely, H., Coops, N.C., White, J.C., Montwe, S.D., Winiwarter, L., Ragab, A., 2023. Modelling tree biomass using direct and additive methods with point cloud deep learning in a temperate mixed forest. Sci. Remote Sens. 8 (2023), 100110 https://doi.org/10.1016/j.srs.2023.100110.

TensorFlow, 2023. Create production-grade machine learning models with TensorFlow. Available at https://www.tensorflow.org/, accessed 10 January 2023.

Terryn, L., Calders, K., Bartholomeus, H., Bartolo, R.E., Brede, B., D'hont, B., Disney, M., Herold, M., Lau, A., Shenkin, A., Whiteside, T.G., Wilkes, P., Verbeeck, H., 2022. Quantifying tropical forest structure through terrestrial and UAV laser scanning fusion in Australian rainforests. Remote Sens. Environ. 271 (2022) 112912, DOI: 10.1016/j.rse.2022.112912.

Walker, S.M., Murray, L., Tepe, T., 2016. Allometric Equation Evaluation Guidance Document. Winrock International, Arlington, VA, USA, 75 pp.

Wang, Z., 2023. Development of ecological management system for planted forest based ELM deep learning algorithm. 3C Empresa. Investigación y pensamiento crítico, 12 (1), 165-184. DOI: 10.17993/3cemp.2023.120151.165-184.

Xu, Q., Lei, X., Zhang, H., 2022. A novel method for approaching the compatibility of tree biomass estimation by multi-task neural networks. For. Ecol. Manage. 508 (2022), 120011.

Xu, D., Shi, Y., Tsang, I.W., Ong, Y.S., Gong, C., Shen, X., 2020. Survey on multi-output learning. IEEE Trans. Neural Networks Learn. Syst. 31 (7), 2409–2429. https://doi.org/10.1109/TNNLS.2019.2945133.

Zhang, H., Bauters, M., Boeckx, P., Van Oost, K., 2021. Mapping canopy heights in dense tropical forests using low-cost UAV-derived photogrammetric point clouds and machine learning approaches. Remote Sens. 2021 (13), 3777. https://doi.org/10.3390/rs13183777.

Zhou, Z.H., Feng, J., 2019. Deep forest. Natl. Sci. Rev. 6, 74–86. https://doi.org/10.1093/nsr/nwy108.